PHYSICAL REVIEW B VOLUME 23, NUMBER 8 15 APRIL 1981

Fluctuation-induced first-order transitions and symmetry-breaking fields. I. Cubic model

Michel Kerszberg and David Mukamel
Department of Nuclear Physics, Weizmann Institute of Science, Rehovot, Israel
(Received 27 August 1980)

A model Hamiltonian for which a stable fixed point is not accessible is expected to yield a first-order transition. By applying a symmetry-breaking field, a continuous transition may be restored. The crossover from first-order to continuous transition induced by the most general quadratic symmetry-breaking field, g, for an $n = 2$ cubic model, is studied using large-g expansion, mean-field, and renormalization-group calculations. It is shown that the (g,T) phase diagram is rather complex, exhibiting tricritical, fourth-order critical, and critical end points. This phase diagram may be realized in certain compounds corresponding to $n = 2$ and $n = 3$ cubic models such as $Tb_2(MoO_4)_3$, $BaTiO_3$, $RbCaF_3$, and $KMnF_3$.

I. INTRODUCTION

First-order phase transitions brought about by the existence of critical fluctuations have been of great interest in recent years.[1-15] Within the renormalization-group framework, this phenomenon manifests itself in the following way. Consider a model Hamiltonian $\mathcal{H}$ which, in the mean-field approximation, yields a second-order transition. Let $\mathcal{H}$ be such that, under renormalization-group transformation, it does not flow to a fixed point, but rather to a region in its parameter space where it becomes thermodynamically unstable. This may be due either to the absence of stable fixed points,[1-7] or to the inaccessibility of existing stable fixed points.[8-10] Such a situation has generally been interpreted as signaling the presence of a first-order transition. Physical systems which are described by model Hamiltonians with no stable fixed point have been studied extensively.[1-7] In these studies one first constructs the Landau-Ginzburg-Wilson (LGW) Hamiltonian which can describe the transition of interest and which embodies the correct symmetries. This Hamiltonian is then studied using renormalization-group techniques in $d = 4 - \epsilon$ dimensions.[16,17] The LGW Hamiltonian associated with a phase transition described by an n-component order parameter is:

$$H = \int \mathcal{H}\, d^d x \,, \tag{1a}$$

$$\mathcal{H} = -\tfrac{1}{2} r \sum_{i=1}^{n} \phi_i^2 - \tfrac{1}{2} \sum_{i=1}^{n} (\nabla \phi_i)^2 - u_1 \Big(\sum_{i=1}^{n} \phi_i^2 \Big)^2 - \sum_{l=2}^{L} u_l O_l(\phi_i) \,, \tag{1b}$$

where r is a temperaturelike variable, $r \sim T - T_0$, and $O_l(\phi_i)$ are fourth-order terms in ϕ_i, which are invariant under the symmetry group of the disordered phase. It has been shown by Brézin, Le Guillou, and Zinn-Justin[18] that the *isotropic fixed point*, characterized by $u_1^* > 0$, $u_2^* = \cdots = u_L^* = 0$, is stable if the order parameter has less than $n^x(d)$ components, with

$$n^x(d) = 4 - 2\epsilon + O(\epsilon^2) \,. \tag{2}$$

For $n > n^x$, the isotropic fixed point becomes unstable to the anisotropic $u_2, \ldots, u_L$ perturbations. The model may or may not possess an anisotropic fixed point depending on the detailed symmetry of the Hamiltonian. It has recently been observed[1-4] that the LGW Hamiltonians appropriate to some real materials (such as MnO, UO_2, Cr, Eu, TbP, and others), for which $n \geq 4$, exhibit no stable fixed point. Thus, even though the Landau theory predicts a second-order transition in these materials, one is led to expect the transitions to be of first order, as indeed is observed experimentally (see, e.g., Ref. 1).

It is also expected that when applying a field which does not break the symmetry of the disordered phase (e.g., hydrostatic pressure), the transition should stay first order. This is due to the fact that the LGW Hamiltonian associated with the transition in the presence of the non-symmetry-breaking field has the same form as the one without a field, and therefore it does not possess a stable fixed point. This prediction has recently been tested experimentally[19] on MnO. It was found that hydrostatic pressure of up to 33 kbars does not change the nature of the transition. However, it has been suggested[11-15] that by applying a symmetry-breaking field, g (such as a magnetic field or a uniaxial stress), the number of components of the effective order parameter can be reduced, and the transition may become second order. This has been verified by Monte Carlo calculations and high-temperature series expansion[14] on a model Hamiltonian appropriate for the phase transition in UO_2. The crossover from first-order to continuous transition has been observed experimentally[20] in MnO when a sufficiently strong uniaxial stress along the [111] direction is applied. It has also been observed in $RbCaF_3$ under a [100]

uniaxial stress.[21]

Models which do not possess a stable fixed point are quite complicated (they usually have a large number of coupling constants). Detailed study of the (g,T) phase diagrams associated with these models has thus not been carried out. Instead, Domany, Mukamel, and Fisher[12] have studied the (g,T) phase diagram of a relatively simple n-component LGW model with cubic anisotropy defined by

$$\mathcal{H}=-\tfrac{1}{2}r\sum_{i=1}^{n}\phi_i^2-\tfrac{1}{2}\sum_{i=1}^{n}(\nabla\phi_i)^2-u\sum_{i=n}^{n}\phi_i^4-v\sum_{i<j}\phi_i^2\phi_j^2. \tag{3a}$$

For stability of the free energy one requires

$$u>0 \tag{3b}$$

and

$$u+\tfrac{1}{2}(n-1)v>0. \tag{3c}$$

This model does have a stable fixed point. For $n<n^x$, the isotropic fixed point is stable in agreement with Brézin *et al.*,[18] while for $n>n^x$ the cubic fixed point becomes stable. However, when examining the flow diagram of the model, one discovers that there exist two regions in the (u,v) plane from which the fixed point is *not accessible*. These regions are (see Fig. 1):

(a) $w>0$,

where

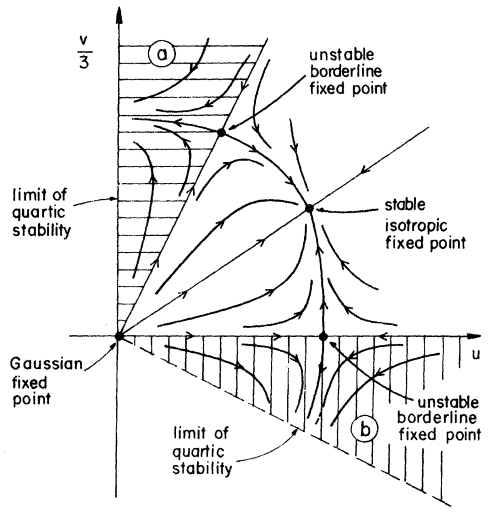

FIG. 1. Schematic renormalization-group flow diagram in the (u,v) plane for the n-component cubic model, with $n<n^x(d)$. The stable isotropic fixed point is not accessible from the two shaded regions marked (a) $w>0$, and (b) $v<0$.

$$w=\begin{cases} v-6u & \text{for } n=2, \\ v-3u+O(\epsilon^2) & \text{for } n=3, \\ v-2u & \text{for } n\geq 4, \end{cases} \tag{4a}$$

and

(b) $v<0$. (4b)

The free energy associated with the Hamiltonian (3) in the regions (4a) and (4b) has been studied by several authors[8-10] who found a first-order phase transition. This result is to be contrasted with the Landau-theory prediction of a continuous transition in the entire stability wedge, as defined by Eqs. (3b) and (3c). Consider now the Hamiltonian (3) which lies in region (a) ($w>0$) and let g_1 be a symmetry-breaking field which enters $\mathcal{H}$ via the term

$$\frac{g_1}{n}\left((n-m)\sum_{i=1}^{m}\phi_i^2-m\sum_{i=m+1}^{n}\phi_i^2\right). \tag{5}$$

For large and positive g_1 the fluctuations of the $(n-m)$ components $\phi_{m+1},\ldots,\phi_n$ are suppressed and the number of fluctuating components of the order parameter is effectively reduced from n to m. The region $w>0$, as defined by Eq. (4a), shrinks as the number of components of the order parameter is decreased. Thus, although the n-component model (with $g_1=0$) lies outside the domain of attraction of its stable fixed point, the effective m-component model (for large and positive g_1) may lie inside the domain of attraction of its own stable fixed point. In this case one should observe a crossover from first order to continuous transition. This situation has been studied in detail in Ref. 12 using large-g_1 expansion and renormalization-group calculations in $d=4-\epsilon$ dimensions. It was found that for sufficiently small g_1 the transition remains first order while for large g_1 it becomes second order. These two segments of the phase-transition line are separated by a tricritical point [see Fig. 2(a)].

In this paper we study the phase diagram associated with the cubic model when more complicated symmetry-breaking fields are applied. In particular, we consider the (g_2,T) phase diagram associated with the model (3) with $n=2$ and $w>0$, where g_2 is a symmetry-breaking field which enters into the Hamiltonian via the term $g_2\phi_1\phi_2$. The easy axis associated with this field lies along the [11] direction in the (ϕ_1,ϕ_2) plane. This anisotropy competes with the quartic terms which favor the [10] or [01] axes. We find that this competition gives rise to a rather complex phase diagram displaying two critical lines, a line of first-order transitions, a critical end point, and a tricritical point [see Fig. 2(b)]. To complete the analysis we

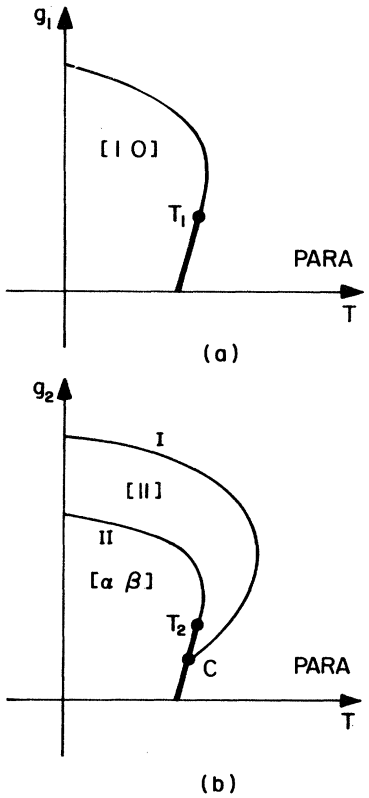

FIG. 2. Schematic (g,T) phase diagrams associated with the $n=2$ cubic model which lies in region (a) of Fig. 1, with symmetry-breaking fields (a) g_1 and (b) g_2 defined by Eqs. (5) and (7), respectively. Thin lines represent continuous transitions, thick lines represent first-order transitions. T_1 and T_2 are tricritical points and C is a critical end point. The direction of the order parameter in the (ϕ_1,ϕ_2) plane is indicated. Note that the discussion in Secs. II and III refers to order parameters which are rotated by 45° with respect to those of the figure.

consider the *most general* symmetry-breaking field which enters into the Hamiltonian via quadratic terms in ϕ_1 and ϕ_2. Such a field can always be written as a linear combination of g_1 and g_2. We find that the (g_1,g_2,T) phase diagram exhibits a fourth-order critical point as shown in Fig. 6. The phase diagram has been studied in the limit of large symmetry-breaking field using perturbation expansion in u and v. In order to substantiate these results we have included a positive sixth-order term in the Hamiltonian (3), and have then studied the phase diagram within the mean-field approximation in a region of the (u,v) plane which is otherwise thermodynamically unstable. The qualitative features of the phase diagram are found to be the same in both methods. A preliminary report of this study has been published elsewhere.[15]

In the following paper we apply the methods developed in the present work in order to study the phase diagrams of several more complicated models corresponding to real physical systems which do not possess a stable fixed point.

The present paper is organized as follows. In Sec. II we analyze the phase diagram of the $n=2$ cubic model in the limit of large anisotropy field. The mean-field approximation is considered in Sec. III. In Sec. IV we discuss several possible physical realizations of the model studied here. The results are summarized in Sec. V.

II. CUBIC MODEL WITH LARGE ANISOTROPY FIELD

A. (g_2,T) phase diagram

Consider the following model Hamiltonian:

$$H=\int \mathcal{H}\,d^dx\,, \tag{6a}$$

with

$$\mathcal{H}=-\tfrac{1}{2}r(\phi_1^2+\phi_2^2)-\tfrac{1}{2}[(\nabla\phi_1)^2+(\nabla\phi_2)^2] -u(\phi_1^4+\phi_2^4)-v\phi_1^2\phi_2^2\,. \tag{6b}$$

For stability of the free energy one requires $u>0$ and $2u+v>0$. Let u and v be such that $w=v-6u>0$. Thus the Hamiltonian lies in region (a) of Fig. 1 [see Eq. (4a)], and it exhibits a first-order transition. Consider now an anisotropy field g_2 which introduces a coupling term

$$g_2\phi_1\phi_2 \tag{7}$$

into the Hamiltonian. It is readily seen, by applying a 45° rotation in the (ϕ_1,ϕ_2) plane, that this problem is equivalent to one which is described by the same Hamiltonian (6), lying, however, in region (b) of Fig. 1 [Eq. (4b)], with a symmetry-breaking field $g_1(\phi_1^2-\phi_2^2)$. For convenience we consider in this section the Hamiltonian

$$\mathcal{H}=-\tfrac{1}{2}r_1\phi_1^2-\tfrac{1}{2}r_2\phi_2^2-\tfrac{1}{2}[(\nabla\phi_1)^2+(\nabla\phi_2)^2] -u(\phi_1^4+\phi_2^4)-v\phi_1^2\phi_2^2\,, \tag{8}$$

with $r_1=r-g$, $r_2=r+g$, and $-2u<v<0$.

The gross features of the (r,g) phase diagram can be found quite easily. At $g=0$ and low temperatures, there exists an ordered phase in which the order parameter lies along the [11] direction in the (ϕ_1,ϕ_2) plane. As discussed in the Introduction, this phase is separated from the disordered phase by a first-order transition. Consider now the ordered phase when a small field g is applied. Owing to the competition between the quadratic and the quartic terms, the order parameter will lie along some direction $[\alpha\beta]$, determined by the strength of g. For large and positive (negative) g, the ϕ_2 (ϕ_1) component is suppressed and the system will order in a phase characterized by an or-

der parameter pointing along the [10] ([01]) direction. The [10] ([01]) phase is expected to be separated from the $[\alpha\beta]$ phase by a phase-transition line at which the order parameter starts rotating away from the [10] ([01]) direction. The two transition lines PARA-[10] and [10]-$[\alpha\beta]$ should be lines of second-order transitions for large g. In this section we study the details of the (r,g) phase diagram. In particular, we analyze the way in which the two transition lines meet, and the various multicritical points which appear in this phase diagram.

Consider the limit of large symmetry-breaking field $g \gtrsim 1$ and $u,v \ll 1$. Furthermore, assume that the Hamiltonian, although stable, is *very close* to the instability limit, namely, $0 < v + 2u \ll O(u,v)$. For $g \gtrsim 1$, there exists a critical line I [Fig. 2(b)] given by $r_1 \simeq O(u,v)$, separating the disordered phase $\langle\phi_1\rangle = \langle\phi_2\rangle = 0$ from a phase where $\langle\phi_2\rangle = 0$ but $\langle\phi_1\rangle \neq 0$. Note that $(\phi_1\phi_2)$ of Fig. 2 are rotated by 45° with respect to those of the Hamiltonian (8). To study the phase transition which occurs inside the ordered phase, we introduce a shift in the order parameter ϕ_1. Define

$$\phi_1 = M + \sigma , \tag{9}$$

with

$$M^2 = |r_1|/4u . \tag{10}$$

The Hamiltonian (8) becomes

$$\mathcal{H} = -\tfrac{1}{2}\bar{r}_1\sigma^2 - \tfrac{1}{2}\bar{r}_2\phi_2^2 - \tfrac{1}{2}[(\nabla\sigma)^2 + (\nabla\phi_2)^2] - w_1\sigma^3 - w_2\sigma\phi_2^2 - u(\sigma^4 + \phi_2^4) - v\sigma^2\phi_2^2 , \tag{11a}$$

where

$$\bar{r}_1 = 2|r_1| , \tag{11b}$$

$$\bar{r}_2 = r_2 + 2vM^2 , \tag{11c}$$

$$w_1 = 4uM , \tag{11d}$$

and

$$w_2 = 2vM . \tag{11e}$$

The choice (10) for M ensures that no term of first order in σ enters into Eq. (11). It is not difficult to show that the considerations which follow are not affected by this choice. We now study the region $r_1 < -1$, deep inside the ordered phase. Clearly, fluctuations of σ become small. Thus we may integrate out the σ field and obtain an effective one-component (Ising-type) Hamiltonian

$$\mathcal{H}_{\text{eff}} = -\tfrac{1}{2}\bar{r}\phi_2^2 - \tfrac{1}{2}(\nabla\phi_2)^2 - u_4\phi_2^4 - u_6\phi_2^6 - \cdots . \tag{12}$$

The coefficients which appear in this expression are evaluated by performing a perturbation expansion in u and v. We find

$$\bar{r} = r_2 - 2vA_1(\bar{r}_1) + O(v^2,u^2) , \tag{13a}$$

$$u_4 = u - \frac{1}{4u}v^2 - 4A_2(\bar{r}_1)v^2 + O(u^3,v^3) , \tag{13b}$$

and

$$u_6 = -\tfrac{32}{3}v^3A_3(\bar{r}_1) + O(u^4,v^4) , \tag{13c}$$

where

$$A_n(x) = \int_{|q|\leq 1} \frac{1}{(x+q^2)^n}\frac{d^dq}{(2\pi)^d} . \tag{14}$$

The diagrams which contribute to u_4 are given in Fig. 3. There are two diagrams which contribute $O(u,v)$ terms and six diagrams which contribute $O(u^2,v^2)$ terms. The diagrams involved in the calculation of u_6 are depicted in Fig. 4. There are two diagrams [Fig. 4(a)] which contribute $O(u^2,v^2)$ terms, but they cancel each other. Therefore the leading contribution to u_6 is of $O(u^3,v^3)$. Of the diagrams listed in Figs. 4(b)–4(d), only those of Fig. 4(b) contribute a nonvanishing term to u_6. Those of Figs. 4(c) and 4(d) cancel each other and their net contribution is zero. Note that in region (b) of Fig. 1, where we work, u_6 is always positive. Now, consider the sign of u_4. In three dimensions or more, (12) yields a continuous transition for $u_4 \gtrsim 0$ [the transition being located at $\bar{r} \simeq O(u_4)$], a first-order transition for $u_4 \lesssim 0$, and a tricritical point at $u_4 = u_{4,t} \simeq O(u_6) = O(v^3)$ and $\bar{r} = \bar{r}_t \simeq O(u_6) = O(v^3)$. To leading order in u and v, the tricritical point is located by solving the equations

$$\bar{r}_t(r,g,u,v) = u_{4,t}(r,g,u,v) = 0 . \tag{15}$$

Taking into account that $A_2(\bar{r}_1)$ is a decreasing

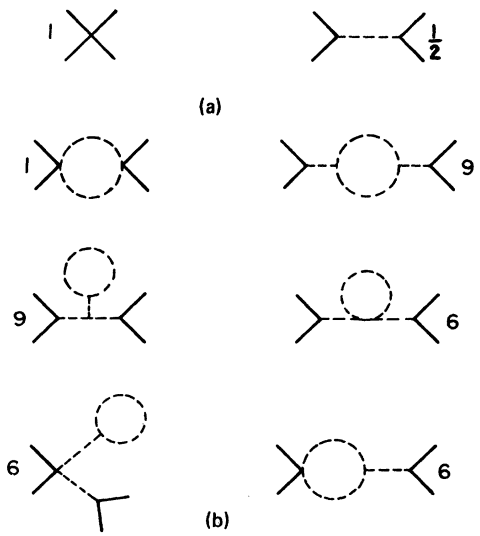

FIG. 3. Diagrams contributing to u_4 [Eq. (13b)]; (a) to $O(u,v)$ and (b) to $O(u^2,v^2)$. The combinatorial factor associated with each diagram is indicated. Dashed lines denote σ propagators and full lines denote ϕ_2 fields.

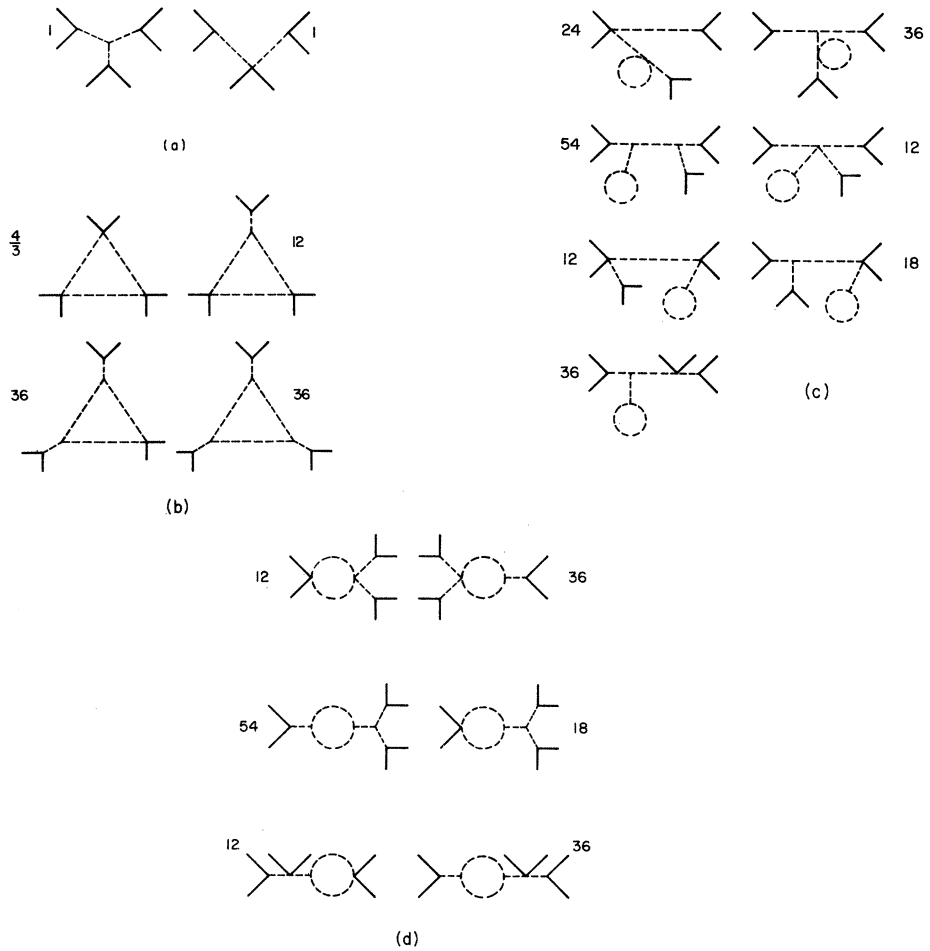

FIG. 4. Diagrams contributing to u_6 [Eq. (13c)], (a) to $O(u^2,v^2)$ and (b), (c), (d) to $O(u^3,v^3)$. The combinatorial factor associated with each diagram is indicated. Dashed lines denote σ propagators and full lines denote ϕ_2 fields. The net contribution of the diagrams (a), (c), and (d) is zero. The only nonvanishing contribution to u_6 comes from diagrams (b).

function of its argument and approaches zero as $\bar{r}_1 \to \infty$, we see that for large $\bar{r}_1 = 2|r-g|$, namely, for large enough g, one has $u_4 > 0$, and the transition is continuous. There will be a tricritical value g_t for which $\bar{r}_{1,t} = 2|r-g_t|$ is such that u_4 vanishes, namely,

$$A_2(\bar{r}_{1,t}) = \tfrac{1}{16}(2-v/u)(2u+v)/v^2 . \tag{16}$$

For $g < g_t$ the transition becomes discontinuous. Note that our approximation is valid only for $\bar{r}_{1,t} \gtrsim 1$ which implies $A_2(\bar{r}_{1,t}) \lesssim O(1)$. Thus, the existence of a tricritical point has been established only for $0 < 2u+v \lesssim v^2$. However, one should notice that, provided we start out in region (b) of Fig. 1, the Hamiltonian (8) will flow, under renormalization-group transformation,[17,22,23] towards the instability limit $2u+v=0$. We therefore expect our result to hold in the entire region (b).

Consider now the PARA-[10] critical line I [Fig. 2(b)]. We will show that one does not expect to find a tricritical point on this line at large g. This can be seen in the following way: Consider the Hamiltonian (8). In the limit of large anisotropy field g, and in the vicinity of the critical line I, one has $r_2 = O(1)$. One can therefore integrate out the ϕ_2 field and obtain an Ising-type effective Hamiltonian for the field ϕ_1:

$$\mathcal{H}_{\text{eff}} = -\tfrac{1}{2} r_{\text{eff}} \phi_1^2 - \tfrac{1}{2}(\nabla\phi_1)^2 - u_{\text{eff}} \phi_1^4 - O(\phi_1^6) , \tag{17a}$$

where u_{eff} is given by

$$u_{\text{eff}} = u - v^2 A_2(r_2) + O(u^3, v^3) . \tag{17b}$$

For $r_2 \gtrsim O(1)$ the integral A_2 satisfies $A_2(r_2) \lesssim O(1)$. Therefore, in region (b), where $v+2u > 0$, one has $u_{\text{eff}} > 0$, and no tricritical point is found on the critical line I at large g. It is, in principle,

possible that this critical line terminates in a tricritical point located at small g (see Fig. 5). However, mean-field analysis, which is described in detail in Sec. III, seems to indicate that the critical line I terminates in a *critical end point* rather than a tricritical point, as shown in Fig. 2(b) [in the mean-field study, we add a positive sixth-order term to the Hamiltonian (8) and study its (g,T) phase diagram outside the stability wedge, namely in the region $v+2u<0$].

B. (g_1,g_2,T) phase diagram

In this section we study the phase diagram associated with the *most general* symmetry-breaking field which enters into the Hamiltonian via quadratic terms in ϕ_i. Such a field can always be written as a linear combination of g_1 and g_2. We thus consider the Hamiltonian:

$$\mathcal{H}=-\tfrac{1}{2}r_1\phi_1^2-\tfrac{1}{2}r_2\phi_2^2-g_2\phi_1\phi_2-\tfrac{1}{2}[(\nabla\phi_1)^2+(\nabla\phi_2)^2] -u(\phi_1^4+\phi_2^4)-v\phi_1^2\phi_2^2\,, \tag{18}$$

where $r_1=r-g_1$ and $r_2=r+g_1$. Since both fields g_1 and g_2 are present in this Hamiltonian, it is immaterial whether the Hamiltonian is located in region (a) or (b) of Fig. 1. In order to study the (g_1, g_2, T) phase diagram associated with the Hamiltonian (18), we first demonstrate the existence of a *fourth-order critical point* at a nonvanishing value of the fields g_1 and g_2. This point is located on the critical surface which separates the paramagnetic and the ordered phases. The various thermodynamic surfaces which appear in the (g_1,T) and (g_2,T) planes can then be connected in a simple way to yield the phase diagram of Fig. 6.

We start by performing a rotation in the (ϕ_1,ϕ_2) plane, which diagonalizes the quadratic terms of the Hamiltonian (18). Define

$$\phi_1=\alpha\psi_1+\beta\psi_2\,, \qquad \phi_2=-\beta\psi_1+\alpha\psi_2\,, \tag{19}$$

with $\alpha^2+\beta^2=1$, $\alpha=\cos\theta$, $\mathrm{tg}2\theta=2g_2/(r_2-r_1)$. The Hamiltonian now takes the form

$$\mathcal{H}=-\tfrac{1}{2}\bar{r}_1\psi_1^2-\tfrac{1}{2}\bar{r}_2\psi_2^2-\tfrac{1}{2}[(\nabla\psi_1)^2+(\nabla\psi_2)^2] -\bar{u}(\psi_1^4+\psi_2^4)-\bar{v}\psi_1^2\psi_2^2-\bar{w}(\psi_1^3\psi_2-\psi_2^3\psi_1)\,, \tag{20a}$$

where

$$\bar{u}=u+(v-2u)\alpha^2(1-\alpha^2)\,, \tag{20b}$$

$$\bar{v}=v+6(2u-v)\alpha^2(1-\alpha^2)\,, \tag{20c}$$

and

$$\bar{w}=2(2u-v)(2\alpha^2-1)\alpha(1-\alpha^2)^{1/2}\,. \tag{20d}$$

Assuming that the symmetry-breaking fields g_1 and g_2 are large we take $\bar{r}_2\simeq O(1)$ near the critical surface $\bar{r}_1\simeq O(\bar{u},\bar{v},\bar{w})$. Integrating out the ψ_2 field we obtain an effective Ising-type Hamiltonian

$$\mathcal{H}_{\mathrm{eff}}=-\tfrac{1}{2}\tilde{r}\psi_1^2-\tfrac{1}{2}(\nabla\psi_1)^2-\tilde{u}_4\psi_1^4-\tilde{u}_6\psi_1^6-\tilde{u}_8\psi_1^8-O(\psi_1^{10})\,, \tag{21}$$

where the coefficients $\tilde{r}$, $\tilde{u}_4$, $\tilde{u}_6$, and $\tilde{u}_8$ can be calculated using a perturbation expansion in $\bar{u}$, $\bar{v}$, and $\bar{w}$, as was done in the preceding section. To leading order in $\bar{u}$, $\bar{v}$, and $\bar{w}$, the fourth-order critical point is located at

$$\tilde{r}(r,g_1,g_2,u,v)=\tilde{u}_4(r,g_1,g_2,u,v) =\tilde{u}_6(r,g_1,g_2,u,v)=0\,, \tag{22}$$

with $\tilde{u}_8>0$. Consider first the coefficient $\tilde{u}_6$:

$$\tilde{u}_6=-\bar{w}^2\frac{1}{2\bar{r}_2}+\tfrac{4}{3}\bar{v}^3A_3(\bar{r}_2)\,, \tag{23}$$

with A_3 defined by Eq. (14). Repeating the reasoning presented in Sec. IIA, we see that the equation $\tilde{u}_6=0$ is satisfied for $\bar{r}_2=O(1)$ only if

$$\bar{w}^2=O(\bar{v}^3)\,. \tag{24}$$

Using the expressions (20c) and (20d) for $\bar{v}$ and $\bar{w}$, we find that Eq. (24) implies

$$2\alpha(2\alpha^2-1)(1-\alpha^2)^{1/2}=\sin4\theta\simeq O(\sqrt{u},\sqrt{|v|})\,, \tag{25}$$

which means that either

$$\theta\simeq O(\sqrt{u},\sqrt{|v|}) \tag{26a}$$

or

$$\theta\simeq\tfrac{1}{4}\pi-O(\sqrt{u},\sqrt{|v|})\,. \tag{26b}$$

We now evaluate $\tilde{u}_4$. To leading order in $\bar{u}$, $\bar{v}$, and $\bar{w}$ we find

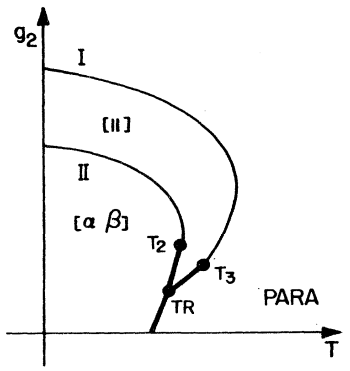

FIG. 5. A possible (g_2,T) phase diagram exhibiting a tricritical point T_3 on the critical line I at small g_2. This diagram also exhibits a triple point TR. Mean-field and renormalization-group considerations indicate that this is *not* the correct phase diagram for the model (8).

$$\tilde{u}_4=\bar{u}-\bar{v}^2A_2(\bar{r}_2)+O(\bar{w}^2)\,. \tag{27}$$

In this expression we have made use of the fact [Eq. (24)] that $\bar{w}^2=O(\bar{v}^3)$. At the fourth-order critical point one has $u_4=0$ and therefore

$$\bar{u}=O(\bar{v}^2)\,, \tag{28a}$$

which reduces, according to whether θ is close to 0 or $\pi/4$, to

$$0<u=O(v^2) \tag{28b}$$

or

$$0<2u+v=O(v^2)\,, \tag{28c}$$

respectively. Therefore, we have demonstrated that the equations $\tilde{u}_4=\tilde{u}_6=0$ may be satisfied near the instability limits of the Hamiltonian (18). We note again that if the initial Hamiltonian lies anywhere in regions (a) or (b), it will flow, under renormalization-group transformation, to the instability limits (28b) and (28c). We therefore expect that one should be able to satisfy the equations $\tilde{u}_4=\tilde{u}_6=0$ in the entire regions (a) or (b) (although not necessarily for large anisotropy fields g_1 and g_2). To conclude, we demonstrate that the fourth-order point is stable, namely, that $\tilde{u}_8>0$ at this point. We find

$$\tilde{u}_8=-\tfrac{2}{3}\bar{v}^4A_4(\bar{r}_2)+\bar{w}^2\bar{v}\frac{1}{\bar{r}_2}\,, \tag{29}$$

which, together with $\tilde{u}_6=0$, yields

$$\tilde{u}_8=\frac{\bar{v}^4}{3}\left(-2A_4(\bar{r}_2)+8\frac{1}{\bar{r}_2}A_3(\bar{r}_2)\right)>0\,. \tag{30}$$

This proves that the fourth-order point found in this section is locally stable.

In order to construct the (g_1,g_2,T) phase diagram we connect, in a simple way, the various thermodynamic surfaces which appear in the (g_1,T) and (g_2,T) planes, taking into account the fact that there exists a fourth-order critical point at nonzero fields g_1 and g_2. In doing so we make use of the detailed study of the phase diagram in the vicinity of a fourth-order critical point, performed previously.[24] The resulting phase diagram is shown in Fig. 6. This phase diagram has a critical surface which separates the paramagnetic and the ordered phases. This surface connects the critical line I of the (g_2,T) plane and the critical line which appears in the (g_1,T) plane. On this surface one finds a tricritical line T_1F and a line of critical end points CF. These two lines join at the fourth-order critical point F. The shaded areas which appear in the figure are coexistence surfaces. The line T_2F is the wing critical line of the tricritical point T_2.

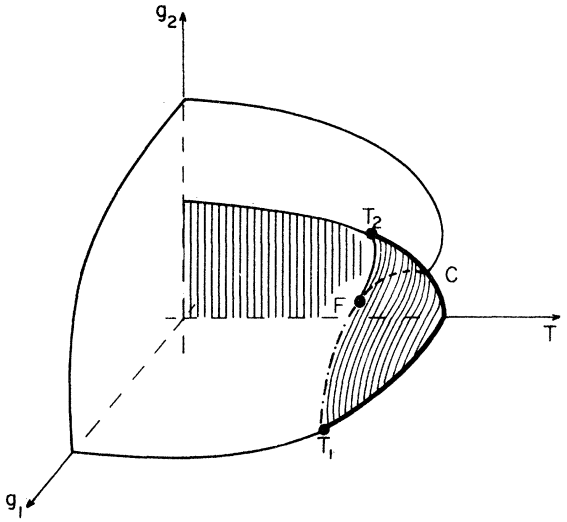

FIG. 6. Schematic (g_1,g_2,T) phase diagram. Thin lines are continuous phase transitions; thick lines and shaded areas are first-order phase transitions, dash-dotted lines are tricritical points, and dashed lines are critical end points. T_1 and T_2 are tricritical points, C is a critical end point, and F is a fourth-order critical point. The line T_2F is the wing critical line associated with tricritical point T_2. The critical lines in the g_1-T, g_2-T, and g_1-g_2 planes and the curve T_1FC form the boundary of a critical surface.

III. MEAN-FIELD APPROXIMATION

Consider the flow diagram associated with the $n=2$ cubic model (Fig. 1). If the initial physical parameters u and v lie in one of the regions (a) or (b) [Eq. (4)], the Hamiltonian flows, under renormalization-group transformation, to a region in its parameter space where it becomes thermodynamically unstable (i.e., either $u<0$ or $v<-2u<0$). In this section we study, in the mean-field approximation, the (g,T) phase diagram associated with the model (8) with $v<-2u<0$. For stability we include in the Hamiltonian a term of sixth order in ϕ_1 and ϕ_2. We therefore consider the Landau Hamiltonian

$$\mathcal{H}_L=\tfrac{1}{2}r_1\phi_1^2+\tfrac{1}{2}r_2\phi_2^2+u(\phi_1^4+\phi_2^2)+v\phi_1^2\phi_2^2+p(\phi_1^2+\phi_2^2)^3\,, \tag{31}$$

where $r_1=r-g$ and $r_2=r+g$ and $p>0$. The phase diagram is symmetric under the transformation $g\to -g$ and therefore we take $g>0$. Since the initial physical Hamiltonian flows to one of the unstable regions, it is expected that the qualitative features of the phase diagram obtained by classical (mean-field) theory *in* the unstable regions should be the same as those obtained by perturbation expansion in the regions (a) or (b) of Fig. (1). We find that the (g,T) phase diagram associated with the Landau model (31) is given by Fig. 2(b),

as suggested by the large-g expansion. In particular, no tricritical point is found on the critical line I. This line terminates in a critical end point.

The order parameter associated with the critical line I is ϕ_1. At the critical line one has $(\partial^2\mathcal{H}_L/\partial\phi_1^2)_{\phi_1=\phi_2=0}=0$, which yields the equation

$$r_1=0 \tag{32}$$

for the critical line I. In order to locate the critical line II, we first find the expectation value of the order parameter in the [10] phase. Setting $\partial\mathcal{H}_L/\partial\phi_1=\partial\mathcal{H}_L/\partial\phi_2=0$, we find

$$\langle\phi_1\rangle=M,\quad \langle\phi_2\rangle=0, \tag{33}$$

where M satisfies the equation

$$r_1+4uM^2+6pM^4=0. \tag{34}$$

The order parameter associated with the critical line II is ϕ_2, and therefore at the critical line one has $(\partial^2\mathcal{H}_L/\partial\phi_2)_{\phi_1=M,\phi_2=0}=0$, which yields

$$r_2+2vM^2+6pM^4=0. \tag{35}$$

Using (34) and (35) we find the following expression for the critical line II:

$$r=-\frac{2u+v}{2u-v}g-6p\frac{1}{(2u-v)^2}g^2. \tag{36}$$

We now show that this critical line terminates in a tricritical point (g_t,r_t). In order to locate the tricritical point, we introduce[24(a)] a small parameter λ defined by

$$\begin{aligned}\phi_2&=\lambda,\\ \phi_1&=M+a\lambda^2,\end{aligned} \tag{37}$$

where a is a constant. Expanding $\mathcal{H}_L$ in power series of λ we find

$$\mathcal{H}_L(\phi_1,\phi_2)=\mathcal{H}_L(M,0)+\tfrac{1}{2}\alpha\lambda^2+\beta\lambda^4+O(\lambda^6), \tag{38}$$

where

$$\alpha=(r_2+2vM^2+6pM^4)+2a(r_1+4uM^2+6pM^4)M \tag{39}$$

and

$$\beta=(4uM^2+12pM^4)a^2+(2vM+12pM^3)a+(u+3pM^2). \tag{40}$$

It is easily seen that at the critical line II [Eqs. (34) and (35)] one has $\alpha=0$. In order to locate the tricritical point, we first minimize β with respect to a. This determines the value of the parameter $a=a_{\min}$. Setting $\beta(a_{\min})=0$ and using Eq. (36) for the critical line one finds an expression for the tricritical point (g_t,r_t). The result is

$$g_t=\frac{v^2-4u^2}{12p} \tag{41a}$$

and

$$r_t=\frac{(2u+v)^2}{24p}. \tag{41b}$$

For $g<g_t$ the transition becomes first order and may be located by finding the solutions of the equations $\partial\mathcal{H}_L/\partial\phi_1=\partial\mathcal{H}_L/\partial\phi_2=0$ and comparing (numerically) the free energy of the various phases.

Consider now the critical line I. We will show that this line terminates in a critical end point. Let

$$\begin{aligned}\phi_1&=\phi\cos\theta,\\ \phi_2&=\phi\sin\theta.\end{aligned} \tag{42}$$

In terms of the polar coordinates (ϕ,θ) the Landau Hamiltonian at the critical line I, namely at $r_1=0$, is:

$$\mathcal{H}_L=\phi^2\{\tfrac{1}{2}r_2\sin^2\theta+[u+\tfrac{1}{4}(v-2u)\sin^2 2\theta]\phi^2+p\phi^4\}. \tag{43}$$

The critical line I is stable as long as $\mathcal{H}_L>0$ for any $\phi\neq0$ and any θ. At a critical end point $\mathcal{H}_L$ satisfies $\mathcal{H}_L(\phi,\theta)\geq0$; however, there exists a solution $(\phi_0\neq0,\theta_0)$ for which $\mathcal{H}_L(\phi_0,\theta_0)=0$. Solving the three equations $\partial\mathcal{H}_L/\partial\phi=0$, $\partial\mathcal{H}_L/\partial\theta=0$, and $\mathcal{H}_L=0$ we find

$$r_2=\frac{1}{2p}\frac{1}{z^2}[u+(v-2u)z^2(1-z^2)], \tag{44a}$$

where

$$z^2=\frac{1}{6}\left[1+\left(\frac{14u-v}{2u-v}\right)^{1/2}\right]. \tag{44b}$$

These equations, together with the equation $r_1=0$ for the critical line I, define the critical end point. Note that in the limit $v\to-2u$ the tricritical and the critical end point [Eqs. (41) and (44), respectively] join at $r=g=0$. For $v>-2u$ this point becomes an ordinary tetracritical point. We have thus demonstrated that the phase diagram associated with the Landau model (31) is given by Fig. 2(b).

IV. PHYSICAL REALIZATIONS

In this section we discuss several physical systems which, we believe, should exhibit the phase diagrams of Figs. 2 and 6. Clearly, any physical system which is described by the $n=2$ cubic model and exhibits a weak first-order phase transition is a suitable candidate. However, we will show that these phase diagrams may also be realized, e.g., by appropriately stressing systems described by n-component cubic models with $n>2$. In particular, we discuss several examples corresponding to $n=3$.

Consider first the improper ferroelectric com-

pound $Tb_2(MoO_4)_3$. This is a tetragonal crystal which exhibits a first-order phase transition at $T_c = 159\,^{\circ}C$ associated with a zone boundary mode, $\vec{q} = (\frac{1}{2}, \frac{1}{2}, 0)$. This transition has been discussed in detail by Dorner *et al.*[25] who found that it is described by an $n = 2$ component order parameter (ϕ_1, ϕ_2). The LGW Hamiltonian associated with this transition has the form

$$\mathcal{H} = -\tfrac{1}{2}r(\phi_1^2 + \phi_2^2) - \tfrac{1}{2}[(\nabla\phi_1)^2 + (\nabla\phi_2)^2] - u(\phi_1^4 + \phi_2^4) - v\phi_1^2\phi_2^2 - \hat{v}\phi_1\phi_2(\phi_1^2 - \phi_2^2) + O(\phi^6)\,. \quad (45)$$

This Hamiltonian possesses an extra fourth-order term, $\hat{v}$, which does not appear in the Hamiltonian (6). However, this term is a redundant variable. By applying an appropriate rotation in the (ϕ_1, ϕ_2) plane, the Hamiltonian (45) can be transformed into a model of the form given by Eq. (6). It has been shown by Dorner *et al.*[25] that the xy component of the stress tensor T, namely T_{xy}, is coupled to the order parameter (ϕ_1, ϕ_2) via term

$$T_{xy}[a\phi_1\phi_2 + b(\phi_1^2 - \phi_2^2)]\,, \quad (46)$$

where a and b are temperature-dependent coupling constants. Therefore, by applying a T_{xy} stress one produces both g_1 and g_2 symmetry-breaking fields. It has been argued[25] that the parameters u, v, and $\hat{v}$ which appear in the Hamiltonian (45) are such that the model lies outside its stability wedge, and that one has to add positive sixth-order terms to stabilize the free energy. However, this should not affect the expected phase diagram (Figs. 2 and 6), as shown in Sec. III, provided the sixth-order terms are almost isotropic. If this is not the case, a more complicated phase diagram is expected.

We now discuss first-order phase transitions described by the $n = 3$ component cubic model. Such transitions occur in many physical systems among which are $BaTiO_3$,[26] $KMnF_3$,[27] $RbCaF_3$,[21] $RbCdF_3$,[28] $TlCdF_3$,[28] and others. To be specific we consider the ferroelectric phase transition in $BaTiO_3$. This compound undergoes a cubic-to-tetragonal phase transition at $T_c \simeq 130\,^{\circ}C$. The order parameter is the polarization vector and it has three components (ϕ_1, ϕ_2, ϕ_3). The LGW Hamiltonian takes the form

$$\mathcal{H} = -\tfrac{1}{2}r\sum_{i=1}^{3}\phi_i^2 - \tfrac{1}{2}\sum_{i=1}^{3}(\nabla\phi_i)^2 - u\sum_{i=1}^{3}\phi_i^4 - v\sum_{i<j}\phi_i^2\phi_j^2 + O(\phi^6)\,. \quad (47)$$

The anisotropy terms u and v are such that the [100] direction is favored (namely $v > 2u$). The stress tensor is coupled to the order parameter via the term

$$a(T_{xx}\phi_1^2 + T_{yy}\phi_2^2 + T_{zz}\phi_3^2) + b(T_{yz}\phi_2\phi_3 + T_{xz}\phi_1\phi_3 + T_{xy}\phi_1\phi_2)\,, \quad (48)$$

where a and b are coupling constants. Therefore by first applying a uniaxial stress along, for example, the z axis ($T_{zz} \neq 0$), one removes the degeneracy between ϕ_3 and (ϕ_1, ϕ_2). Taking a stress (either tensile or compressive) which favors the $n = 2$ components (ϕ_1, ϕ_2), the fluctuations of the ϕ_3 component are suppressed and one is left with an effective $n = 2$ component cubic model. The g_1 and g_2 symmetry-breaking fields are now realized by applying a uniaxial T_{xx} or a shear T_{xy} stress, respectively. Both fields may be realized by applying a uniaxial stress in a general direction in the xy plane as well. These symmetry considerations also apply to $KMnF_3$, $RbCaF_3$, $RbCdF_3$, and $TlCdF_3$.

The phase diagram of $RbCaF_3$ under uniaxial [100] stress (T_{xx}) has recently been studied experimentally.[21] It was found that the system exhibits a tricritical point as indicated by the (g_1, T) phase diagram [Fig. 2(a)]. It is therefore suggested that if in addition to the compressive T_{xx} stress, one applies a shear component T_{xy}, the (g_2, T) phase diagram can be mapped out. Note however, that the dispersion relation in $RbCaF_3$ and $KMnF_3$ is strongly anisotropic,[21] suggesting that a crossover to a Lifshitz-type behavior[29] should occur in these systems. Again, this may complicate the phase diagram.

V. CONCLUDING REMARKS

In this paper we have studied first-order phase transitions associated with *inaccessibility of a stable fixed point*. It had previously been argued that by applying a symmetry-breaking field, g, such a transition may become continuous. This crossover from first order to continuous transition induced by symmetry-breaking fields has been studied in detail in the present work. More specifically we considered the LGW model with cubic anisotropy. This model exhibits a fluctuation-induced first-order transition in certain regions of its parameter space. The *phase diagram* associated with the *most general* quadratic symmetry-breaking field for the $n = 2$ cubic model, has been determined. We found that the crossover from first-order to continuous transition occurs in quite a complicated fashion, through a series of multicritical points including tricritical, fourth-order critical, and critical end points. The complete phase diagram is given in Figs. 2 and 6. Our results are based on large anisotropy field expansions combined with mean-field and renormalization-group calculations.

It is suggested that the interesting crossover found in this work may be observed in certain compounds exhibiting structural transitions such as $Tb_2(MoO_4)_3$, $BaTiO_3$, $KMnF_3$, $RbCaF_3$, $RbCdF_3$, and others. These physical systems are described by $n=2$ and $n=3$ cubic models. We believe it would be of great interest to test the predictions of this study in these compounds.

In the following paper we apply the methods derived in this work in order to study the phase diagrams associated with physical systems described by LGW models with *no stable fixed point*. These LGW models involve a large number of fourth-order invariants, and the (g,T) phase diagram is expected to be rather complex.

ACKNOWLEDGMENTS

This work was supported in part by a grant from the U.S.-Israel Binational Science Foundation, Jerusalem, Israel and by Keren Bat-Sheva de Rothschild.

[1]D. Mukamel and S. Krinsky, Phys. Rev. B 13, 5065 (1976); 13, 5078 (1976); P. Bak and D. Mukamel, *ibid.*, 13, 5086 (1976).
[2]P. Bak, S. Krinsky, and D. Mukamel, Phys. Rev. Lett. 36, 52 (1976).
[3]S. A. Brazovskii and I. E. Dzyaloshinskii, Zh. Eksp. Teor. Fiz. Pis'ma Red. 21, 360 (1975) [JETP Lett. 21, 164 (1975)].
[4]I. E. Dzyaloshinskii, Zh. Eksp. Teor. Fiz. 72, 1930 (1977) [Sov. Phys.—JETP 45, 1014 (1977)].
[5]V. A. Alessandrini, A. P. Cracknell, and J. A. Przystawa, Commun. Phys. 1, 51 (1976).
[6]D. Mukamel and D. J. Wallace, J. Phys. C 13, L851 (1979); 13, L139 (1980).
[7]O. G. Mouritsen, S. J. Knak Jensen, and P. Bak, Phys. Rev. Lett. 39, 629 (1977).
[8]T. Nattermann and S. Trimper, J. Phys. A 8, 2000 (1975); T. Nattermann, J. Phys. C 9, 3337 (1976).
[9]J. Rudnick, Phys. Rev. B 18, 1406 (1978).
[10]I. F. Lyuksyutov and V. Pokrovskii, Zh. Eksp. Teor. Fiz. Pis'ma Red. 21, 22 (1975) [JETP Lett. 21, 9 (1975)].
[11]P. Bak, S. Krinsky, and D. Mukamel, Phys. Rev. Lett. 36, 829 (1976).
[12]E. Domany, D. Mukamel, and M. E. Fisher, Phys. Rev. B 15, 5432 (1977).
[13]J. Solyom and G. S. Grest, Phys. Rev. B 16, 2235 (1977).
[14]S. J. Knak Jensen, O. G. Mouritsen, E. K. Hansen, and P. Bak, Phys. Rev. B 19, 5886 (1979).
[15]M. Kerszberg and D. Mukamel, Phys. Rev. Lett. 43, 293 (1979).
[16]See, e.g., (a) K. G. Wilson and J. B. Kogut, Phys. Rep. 12C, 75 (1974); (b) *Phase Transitions and Critical Phenomena*, edited by C. Domb and M. S. Green (Academic, New York, 1976), Vol. VI.
[17]For a discussion of the renormalization group flows of the cubic model see, e.g., A. Aharony in Ref. 16 (b).
[18]E. Brézin, J. C. Le Guillou, and J. Zinn-Justin, Phys. Rev. B 10, 892 (1974).
[19]D. Bloch, C. Vettier, and P. Burlet, Phys. Lett. 75A, 301 (1980).
[20]D. Bloch, D. Hermann-Ronzaud, C. Vettier, W. B. Yelon, and R. Alben, Phys. Rev. Lett. 35, 963 (1975).
[21]A. Aharony and A. D. Bruce, Phys. Rev. Lett. 42, 462 (1979); J. Y. Buzaré, J. C. Fayet, W. Berlinger, and K. A. Muller, *ibid.* 42, 465 (1979).
[22]J. Rudnick and D. R. Nelson, Phys. Rev. B 13, 2208 (1976).
[23]D. R. Nelson and E. Domany, Phys. Rev. B 13, 236 (1976); E. Domany, D. R. Nelson, and M. E. Fisher, *ibid.* 15, 3453 (1977); E. Domany and M. E. Fisher, *ibid.* 15, 3510 (1977).
[24](a) S. Krinsky and D. Mukamel, Phys. Rev. B 11, 399 (1975); 12, 211 (1975); (b) M. Kerszberg, D. Mukamel, H. Rohrer, and H. Thomas, J. Appl. Phys. 50, 1836 (1979).
[25]B. Dorner, J. D. Axe, and G. Shirane, Phys. Rev. B 6, 1950 (1972).
[26]A. F. Devonshire, Adv. Phys. 3, 85 (1954).
[27]G. Shirane, V. J. Minkiewicz, and A. Linz, Solid State Commun. 8, 1941 (1970).
[28]M. Rousseau, J. Y. Gesland, J. Julliard, J. Nouet, J. Zarembowitch, and A. Zarembowitch, J. Phys. (Paris) 36, L-121 (1975).
[29]R. M. Hornreich, M. Luban, and S. Shtrikman, Phys. Rev. Lett. 35, 1678 (1975).